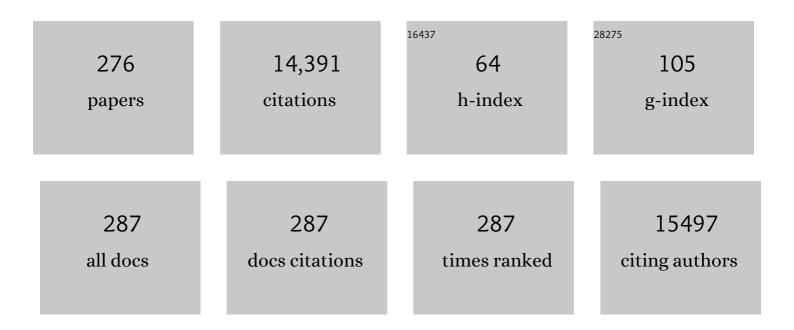
## Victor S Batista

List of Publications by Year in descending order

Source: https://exaly.com/author-pdf/3957525/publications.pdf Version: 2024-02-01



#	Article	IF	CITATIONS
1	Distinct allosteric pathways in imidazole glycerol phosphate synthase from yeast and bacteria. Biophysical Journal, 2022, 121, 119-130.	0.2	8
2	Binding of the substrate analog methanol in the oxygen-evolving complex of photosystem II in the D1-N87A genetic variant of cyanobacteria. Faraday Discussions, 2022, 234, 195-213.	1.6	4
3	Protein nanowires with tunable functionality and programmable self-assembly using sequence-controlled synthesis. Nature Communications, 2022, 13, 829.	5.8	30
4	High-resolution cryo-electron microscopy structure of photosystem II from the mesophilic cyanobacterium, <i>Synechocystis</i> sp. PCC 6803. Proceedings of the National Academy of Sciences of the United States of America, 2022, 119, .	3.3	58
5	Insights into Binding of Single-Stranded Viral RNA Template to the Replication–Transcription Complex of SARS-CoV-2 for the Priming Reaction from Molecular Dynamics Simulations. Biochemistry, 2022, 61, 424-432.	1.2	10
6	MptpA Kinetics Enhanced by Allosteric Control of an Active Conformation. Journal of Molecular Biology, 2022, 434, 167540.	2.0	7
7	Functional Tensor-Train Chebyshev Method for Multidimensional Quantum Dynamics Simulations. Journal of Chemical Theory and Computation, 2022, 18, 25-36.	2.3	10
8	Glycerol binding at the narrow channel of photosystem II stabilizes the low-spin S2 state of the oxygen-evolving complex. Photosynthesis Research, 2022, , 1.	1.6	1
9	Structural Basis for Reduced Dynamics of Three Engineered HNH Endonuclease Lys-to-Ala Mutants for the Clustered Regularly Interspaced Short Palindromic Repeat (CRISPR)-Associated 9 (CRISPR/Cas9) Enzyme. Biochemistry, 2022, 61, 785-794.	1.2	12
10	A 300-fold conductivity increase in microbial cytochrome nanowires due to temperature-induced restructuring of hydrogen bonding networks. Science Advances, 2022, 8, eabm7193.	4.7	28
11	Tensor-Train Split-Operator KSL (TT-SOKSL) Method for Quantum Dynamics Simulations. Journal of Chemical Theory and Computation, 2022, 18, 3327-3346.	2.3	9
12	Selective Heterogeneous Transfer Hydrogenation from Tertiary Amines to Alkynes. ACS Catalysis, 2021, 11, 5405-5415.	5.5	4
13	Tuning the Conduction Band for Interfacial Electron Transfer: Dye-Sensitized Sn <sub><i>x</i></sub> Ti <sub>1–<i>x</i></sub> O <sub>2</sub> Photoanodes for Water Splitting. ACS Applied Energy Materials, 2021, 4, 4695-4703.	2.5	4
14	Is Deprotonation of the Oxygen-Evolving Complex of Photosystem II during the S <sub>1</sub> → S <sub>2</sub> Transition Suppressed by Proton Quantum Delocalization?. Journal of the American Chemical Society, 2021, 143, 8324-8332.	6.6	21
15	Iterative Power Algorithm for Global Optimization with Quantics Tensor Trains. Journal of Chemical Theory and Computation, 2021, 17, 3280-3291.	2.3	8
16	Introducing special issue on photocatalysis and photoelectrochemistry. Journal of Chemical Physics, 2021, 154, 190401.	1.2	0
17	Mechanism of Inhibition of the Reproduction of SARS-CoV-2 and <i>Ebola</i> Viruses by Remdesivir. Biochemistry, 2021, 60, 1869-1875.	1.2	12
18	Do crystallographic XFEL data support binding of a water molecule to the oxygen-evolving complex of photosystem II exposed to two flashes of light?. Proceedings of the National Academy of Sciences of the United States of America, 2021, 118, .	3.3	11

#	Article	IF	CITATIONS
19	Proton exit pathways surrounding the oxygen evolving complex of photosystem II. Biochimica Et Biophysica Acta - Bioenergetics, 2021, 1862, 148446.	0.5	30
20	Observation of a potential-dependent switch of water-oxidation mechanism on Co-oxide-based catalysts. CheM, 2021, 7, 2101-2117.	5.8	42
21	Distorted Copper(II) Complex with Unusually Short CF···Cu Distances. Inorganic Chemistry, 2021, 60, 14759-14764.	1.9	1
22	A structurally preserved allosteric site in the MIF superfamily affects enzymatic activity and CD74 activation in D-dopachrome tautomerase. Journal of Biological Chemistry, 2021, 297, 101061.	1.6	7
23	Computational insights into the membrane fusion mechanism of SARS-CoV-2 at the cellular level. Computational and Structural Biotechnology Journal, 2021, 19, 5019-5028.	1.9	10
24	Vibrational Stark shift spectroscopy of catalysts under the influence of electric fields at electrode–solution interfaces. Chemical Science, 2021, 12, 10131-10149.	3.7	25
25	Community Network Analysis of Allosteric Proteins. Methods in Molecular Biology, 2021, 2253, 137-151.	0.4	15
26	Intrinsic electronic conductivity of individual atomically resolved amyloid crystals reveals micrometer-long hole hopping via tyrosines. Proceedings of the National Academy of Sciences of the United States of America, 2021, 118, .	3.3	45
27	Nanotechnology for catalysis and solar energy conversion. Nanotechnology, 2021, 32, 042003.	1.3	44
28	Heterogeneous Composition of Oxygen-Evolving Complexes in Crystal Structures of Dark-Adapted Photosystem II. Biochemistry, 2021, 60, 3374-3384.	1.2	8
29	Development of an Enantioselective Synthesis of (â^')-Euonyminol. Journal of Organic Chemistry, 2021, 86, 17011-17035.	1.7	6
30	Enhanced specificity mutations perturb allosteric signaling in CRISPR-Cas9. ELife, 2021, 10, .	2.8	27
31	Copper-mediated thiol potentiation and mutagenesis-guided modeling suggest a highly conserved copper-binding motif in human OR2M3. Cellular and Molecular Life Sciences, 2020, 77, 2157-2179.	2.4	29
32	Allosteric Motions of the CRISPR–Cas9 HNH Nuclease Probed by NMR and Molecular Dynamics. Journal of the American Chemical Society, 2020, 142, 1348-1358.	6.6	78
33	NMR and computational methods for molecular resolution of allosteric pathways in enzyme complexes. Biophysical Reviews, 2020, 12, 155-174.	1.5	35
34	Multihole water oxidation catalysis on haematite photoanodes revealed by operando spectroelectrochemistry and DFT. Nature Chemistry, 2020, 12, 82-89.	6.6	189
35	Ring-polymer, centroid, and mean-field approximations to multi-time Matsubara dynamics. Journal of Chemical Physics, 2020, 153, 124112.	1.2	11
36	Vibronic Dynamics of Photodissociating ICN from Simulations of Ultrafast Xâ€Ray Absorption Spectroscopy. Angewandte Chemie - International Edition, 2020, 59, 20044-20048.	7.2	5

#	Article	IF	CITATIONS
37	Regulation of MIF Enzymatic Activity by an Allosteric Site at the Central Solvent Channel. Cell Chemical Biology, 2020, 27, 740-750.e5.	2.5	20
38	Vibronic Dynamics of Photodissociating ICN from Simulations of Ultrafast Xâ€Ray Absorption Spectroscopy. Angewandte Chemie, 2020, 132, 20219-20223.	1.6	3
39	Two-dimensional Raman spectroscopy of Lennard-Jones liquids via ring-polymer molecular dynamics. Journal of Chemical Physics, 2020, 153, 034117.	1.2	9
40	D1-S169A substitution of photosystem II reveals a novel S2-state structure. Biochimica Et Biophysica Acta - Bioenergetics, 2020, 1861, 148301.	0.5	4
41	A conductive metal–organic framework photoanode. Chemical Science, 2020, 11, 9593-9603.	3.7	16
42	<i>In Situ</i> Identification of Reaction Intermediates and Mechanistic Understandings of Methane Oxidation over Hematite: A Combined Experimental and Theoretical Study. Journal of the American Chemical Society, 2020, 142, 17119-17130.	6.6	59
43	Electric field stimulates production of highly conductive microbial OmcZ nanowires. Nature Chemical Biology, 2020, 16, 1136-1142.	3.9	112
44	Efficient Multiphoton Sampling of Molecular Vibronic Spectra on a Superconducting Bosonic Processor. Physical Review X, 2020, 10, .	2.8	73
45	The Effect of (â~)-Epigallocatechin-3-Gallate on the Amyloid-β Secondary Structure. Biophysical Journal, 2020, 119, 349-359.	0.2	18
46	Semiconductor-to-conductor transition in 2D copper( <scp>ii</scp> ) oxide nanosheets through surface sulfur-functionalization. Nanoscale, 2020, 12, 14549-14559.	2.8	6
47	Surprisingly big linker-dependence of activity and selectivity in CO <sub>2</sub> reduction by an iridium( <scp>i</scp> ) pincer complex. Chemical Communications, 2020, 56, 9126-9129.	2.2	10
48	Identification of a Na <sup>+</sup> -Binding Site near the Oxygen-Evolving Complex of Spinach Photosystem II. Biochemistry, 2020, 59, 2823-2831.	1.2	5
49	Robust Binding of Disulfide-Substituted Rhenium Bipyridyl Complexes for CO2 Reduction on Gold Electrodes. Frontiers in Chemistry, 2020, 8, 86.	1.8	7
50	Decelerating Charge Recombination Using Fluorinated Porphyrins in <i>N,N</i> -Bis(3,4,5-trimethoxyphenyl)aniline—Aluminum(III) Porphyrin—Fullerene Reaction Center Models. Journal of the American Chemical Society, 2020, 142, 10008-10024.	6.6	33
51	Allosteric Impact of the Variable Insert Loop in <i>Vaccinia</i> H1-Related (VHR) Phosphatase. Biochemistry, 2020, 59, 1896-1908.	1.2	5
52	Decrypting the Information Exchange Pathways across the Spliceosome Machinery. Journal of the American Chemical Society, 2020, 142, 8403-8411.	6.6	35
53	Allosteric Control of Enzyme Activity: From Ancient Origins to Recent Gene-Editing Technologies. Biochemistry, 2020, 59, 1711-1712.	1.2	3
54	Facet-Dependent Kinetics and Energetics of Hematite for Solar Water Oxidation Reactions. ACS Applied Materials & Interfaces, 2019, 11, 5616-5622.	4.0	46

#	Article	IF	CITATIONS
55	Catalytic manganese oxide nanostructures for the reverse water gas shift reaction. Nanoscale, 2019, 11, 16677-16688.	2.8	31
56	The <i>JPC</i> Periodic Table. Journal of Physical Chemistry A, 2019, 123, 5837-5848.	1.1	2
57	The <i>JPC</i> Periodic Table. Journal of Physical Chemistry B, 2019, 123, 5973-5984.	1.2	1
58	The <i>JPC</i> Periodic Table. Journal of Physical Chemistry C, 2019, 123, 17063-17074.	1.5	1
59	The <i>JPC</i> Periodic Table. Journal of Physical Chemistry Letters, 2019, 10, 4051-4062.	2.1	2
60	Multi-time formulation of Matsubara dynamics. Journal of Chemical Physics, 2019, 151, 034108.	1.2	14
61	Thermodynamics of the S <sub>2</sub> -to-S <sub>3</sub> state transition of the oxygen-evolving complex of photosystem II. Physical Chemistry Chemical Physics, 2019, 21, 20840-20848.	1.3	21
62	Strongly Coupled Phenazine–Porphyrin Dyads: Light-Harvesting Molecular Assemblies with Broad Absorption Coverage. ACS Applied Materials & Interfaces, 2019, 11, 8000-8008.	4.0	36
63	D1-S169A Substitution of Photosystem II Perturbs Water Oxidation. Biochemistry, 2019, 58, 1379-1387.	1.2	18
64	Hammett neural networks: prediction of frontier orbital energies of tungsten–benzylidyne photoredox complexes. Chemical Science, 2019, 10, 6844-6854.	3.7	13
65	Chiral Inversion of Amino Acids in Antiparallel β-Sheets at Interfaces Probed by Vibrational Sum Frequency Generation Spectroscopy. Journal of Physical Chemistry B, 2019, 123, 5769-5781.	1.2	20
66	Vibronic Effects in the Ultrafast Interfacial Electron Transfer of Perylene-Sensitized TiO <sub>2</sub> Surfaces. Journal of Physical Chemistry C, 2019, 123, 12599-12607.	1.5	15
67	Heterogenized Molecular Catalysts: Vibrational Sum-Frequency Spectroscopic, Electrochemical, and Theoretical Investigations. Accounts of Chemical Research, 2019, 52, 1289-1300.	7.6	53
68	Search for Catalysts by Inverse Design: Artificial Intelligence, Mountain Climbers, and Alchemists. Chemical Reviews, 2019, 119, 6595-6612.	23.0	142
69	Regioselective Ultrafast Photoinduced Electron Transfer from Naphthols to Halocarbon Solvents. Journal of Physical Chemistry Letters, 2019, 10, 2657-2662.	2.1	10
70	Effect of Electronic Coupling on Electron Transfer Rates from Photoexcited Naphthalenediimide Radical Anion to Re(bpy)(CO) <sub>3</sub> X. Journal of Physical Chemistry C, 2019, 123, 10178-10190.	1.5	10
71	Water Network Dynamics Next to the Oxygen-Evolving Complex of Photosystem II. Inorganics, 2019, 7, 39.	1.2	15
72	Collaboration between experiment and theory in solar fuels research. Chemical Society Reviews, 2019, 48, 1865-1873.	18.7	17

#	Article	IF	CITATIONS
73	Exploring Allosteric Pathways of a V-Type Enzyme with Dynamical Perturbation Networks. Journal of Physical Chemistry B, 2019, 123, 3452-3461.	1.2	29
74	Relative stability of the S2 isomers of the oxygen evolving complex of photosystem II. Photosynthesis Research, 2019, 141, 331-341.	1.6	18
75	Atmospheric $\hat{I}^2$ -Caryophyllene-Derived Ozonolysis Products at Interfaces. ACS Earth and Space Chemistry, 2019, 3, 158-169.	1.2	10
76	High-Energy Charge-Separated States by Reductive Electron Transfer Followed by Electron Shift in the Tetraphenylethylene–Aluminum(III) Porphyrin–Fullerene Triad. Journal of Physical Chemistry C, 2019, 123, 131-143.	1.5	24
77	Photoexcited radical anion super-reductants for solar fuels catalysis. Coordination Chemistry Reviews, 2018, 361, 98-119.	9.5	49
78	Floquet Study of Quantum Control of the Cis–Trans Photoisomerization of Rhodopsin. Journal of Chemical Theory and Computation, 2018, 14, 1198-1205.	2.3	10
79	Nitrogen-doped tungsten carbide nanoarray as an efficient bifunctional electrocatalyst for water splitting in acid. Nature Communications, 2018, 9, 924.	5.8	571
80	Stable iridium dinuclear heterogeneous catalysts supported on metal-oxide substrate for solar water oxidation. Proceedings of the National Academy of Sciences of the United States of America, 2018, 115, 2902-2907.	3.3	229
81	Nanosecond Dynamics Regulate the MIFâ€induced Activity of CD74. Angewandte Chemie - International Edition, 2018, 57, 7116-7119.	7.2	32
82	Molecular mechanism of activation of human musk receptors OR5AN1 and OR1A1 by ( <i>R</i> ) Tj ETQq0 0 0 Sciences of the United States of America, 2018, 115, E3950-E3958.	rgBT /Overl 3.3	ock 10 Tf 50 57
83	Direct Interfacial Electron Transfer from High-Potential Porphyrins into Semiconductor Surfaces: A Comparison of Linkers and Anchoring Groups. Journal of Physical Chemistry C, 2018, 122, 13529-13539.	1.5	31
84	Investigating the Role of Copper Oxide in Electrochemical CO <sub>2</sub> Reduction in Real Time. ACS Applied Materials & Interfaces, 2018, 10, 8574-8584.	4.0	207
85	Active sites of copper-complex catalytic materials for electrochemical carbon dioxide reduction. Nature Communications, 2018, 9, 415.	5.8	527
86	Hydrophobic CuO Nanosheets Functionalized with Organic Adsorbates. Journal of the American Chemical Society, 2018, 140, 1824-1833.	6.6	59
87	Can TDDFT Describe Excited Electronic States of Naphthol Photoacids? A Closer Look with EOM-CCSD. Journal of Chemical Theory and Computation, 2018, 14, 867-876.	2.3	27
88	Classical Optimal Control for Energy Minimization Based On Diffeomorphic Modulation under Observable-Response-Preserving Homotopy. Journal of Chemical Theory and Computation, 2018, 14, 3351-3362.	2.3	4
89	Phenothiazine Radical Cation Excited States as Super-oxidants for Energy-Demanding Reactions. Journal of the American Chemical Society, 2018, 140, 5290-5299.	6.6	89
90	Carbon chain shape selectivity by the mouse olfactory receptor OR-17. Organic and Biomolecular Chemistry, 2018, 16, 2541-2548.	1.5	10

#	Article	IF	CITATIONS
91	Dopant-Dependent SFG Response of Rhenium CO <sub>2</sub> Reduction Catalysts Chemisorbed on SrTiO <sub>3</sub> (100) Single Crystals. Journal of Physical Chemistry C, 2018, 122, 13944-13952.	1.5	10
92	Mechanistic study of CO/CO 2 conversion catalyzed by a biomimetic Ni(II)â€iminothiolate complex. International Journal of Quantum Chemistry, 2018, 118, e25555.	1.0	2
93	Electron–Hole-Pair-Induced Vibrational Energy Relaxation of Rhenium Catalysts on Gold Surfaces. Journal of Physical Chemistry Letters, 2018, 9, 406-412.	2.1	22
94	Inverse Design of a Catalyst for Aqueous CO/CO <sub>2</sub> Conversion Informed by the Ni <sup>II</sup> –Iminothiolate Complex. Inorganic Chemistry, 2018, 57, 15474-15480.	1.9	13
95	CO <sub>2</sub> Reduction Catalysts on Gold Electrode Surfaces Influenced by Large Electric Fields. Journal of the American Chemical Society, 2018, 140, 17643-17655.	6.6	103
96	Eigenvector centrality for characterization of protein allosteric pathways. Proceedings of the National Academy of Sciences of the United States of America, 2018, 115, E12201-E12208.	3.3	145
97	Reduced Occupancy of the Oxygen-Evolving Complex of Photosystem II Detected in Cryo-Electron Microscopy Maps. Biochemistry, 2018, 57, 5925-5929.	1.2	3
98	The structural basis for cancer drug interactions with the catalytic and allosteric sites of SAMHD1. Proceedings of the National Academy of Sciences of the United States of America, 2018, 115, E10022-E10031.	3.3	30
99	Distinct Binding of Rhenium Catalysts on Nanostructured and Single-Crystalline TiO <sub>2</sub> Surfaces Revealed by Two-Dimensional Sum Frequency Generation Spectroscopy. Journal of Physical Chemistry C, 2018, 122, 26018-26031.	1.5	8
100	Unusual Stability of a Bacteriochlorin Electrocatalyst under Reductive Conditions. A Case Study on CO <sub>2</sub> Conversion to CO. ACS Catalysis, 2018, 8, 10131-10136.	5.5	28
101	Key role of the REC lobe during CRISPR–Cas9 activation by â€~sensing', â€~regulating', and â€~lockingâ€ catalytic HNH domain. Quarterly Reviews of Biophysics, 2018, 51, .	€™ the 2.4	79
102	A Multispecific Investigation of the Metal Effect in Mammalian Odorant Receptors for Sulfur-Containing Compounds. Chemical Senses, 2018, 43, 357-366.	1.1	7
103	Ultrafast proton-assisted tunneling through ZrO <sub>2</sub> in dye-sensitized SnO <sub>2</sub> -core/ZrO <sub>2</sub> -shell films. Chemical Communications, 2018, 54, 7971-7974.	2.2	5
104	End-On Bound Iridium Dinuclear Heterogeneous Catalysts on WO <sub>3</sub> for Solar Water Oxidation. ACS Central Science, 2018, 4, 1166-1172.	5.3	69
105	Inclusion of nuclear quantum effects for simulations of nonlinear spectroscopy. Journal of Chemical Physics, 2018, 148, 244105.	1.2	16
106	Water-Nucleophilic Attack Mechanism for the Cu <sup>II</sup> (pyalk) <sub>2</sub> Water-Oxidation Catalyst. ACS Catalysis, 2018, 8, 7952-7960.	5.5	37
107	Nanosecond Dynamics Regulate the MIFâ€Induced Activity of CD74. Angewandte Chemie, 2018, 130, 7234-7237.	1.6	2
108	Behavior of Ru–bda Waterâ€Oxidation Catalysts in Low Oxidation States. Chemistry - A European Journal, 2018, 24, 12838-12847.	1.7	27

#	Article	IF	CITATIONS
109	Orientations of nonlocal vibrational modes from combined experimental and theoretical sum frequency spectroscopy. Chemical Physics Letters, 2017, 683, 199-204.	1.2	8
110	Energetics of the S <sub>2</sub> State Spin Isomers of the Oxygen-Evolving Complex of Photosystem II. Journal of Physical Chemistry B, 2017, 121, 1020-1025.	1.2	38
111	Insights into Photosystem II from Isomorphous Difference Fourier Maps of Femtosecond X-ray Diffraction Data and Quantum Mechanics/Molecular Mechanics Structural Models. ACS Energy Letters, 2017, 2, 397-407.	8.8	16
112	Electrochemical Reduction of CO <sub>2</sub> Catalyzed by Re(pyridine-oxazoline)(CO) <sub>3</sub> Cl Complexes. Inorganic Chemistry, 2017, 56, 3214-3226.	1.9	48
113	Photoinduced electron transfer from rylenediimide radical anions and dianions to Re(bpy)(CO) <sub>3</sub> using red and near-infrared light. Chemical Science, 2017, 8, 3821-3831.	3.7	57
114	Altering the allosteric pathway in IGPS suppresses millisecond motions and catalytic activity. Proceedings of the National Academy of Sciences of the United States of America, 2017, 114, E3414-E3423.	3.3	55
115	Inferring Protonation States of Hydroxamate Adsorbates on TiO <sub>2</sub> Surfaces. Journal of Physical Chemistry C, 2017, 121, 11985-11990.	1.5	5
116	The role of metals in mammalian olfaction of low molecular weight organosulfur compounds. Natural Product Reports, 2017, 34, 529-557.	5.2	33
117	Ultrafast photo-induced charge transfer of 1-naphthol and 2-naphthol to halocarbon solvents. Chemical Physics Letters, 2017, 683, 49-56.	1.2	8
118	Mechanistic Insights into Surface Chemical Interactions between Lithium Polysulfides and Transition Metal Oxides. Journal of Physical Chemistry C, 2017, 121, 14222-14227.	1.5	86
119	Antimony Complexes for Electrocatalysis: Activity of a Mainâ€Group Element in Proton Reduction. Angewandte Chemie - International Edition, 2017, 56, 9111-9115.	7.2	51
120	Interfacial Electron Transfer Followed by Photooxidation in <i>N</i> , <i>N</i> -Bis( <i>p</i> -anisole)aminopyridine–Aluminum(III) Porphyrin–Titanium(IV) Oxide Self-Assembled Photoanodes. Journal of Physical Chemistry C, 2017, 121, 14484-14497.	1.5	12
121	Probing the remarkable thermal kinetics of visual rhodopsin with E181Q and S186A mutants. Journal of Chemical Physics, 2017, 146, 215104.	1.2	6
122	Effects of aligned αâ€helix peptide dipoles on experimental electrostatic potentials. Protein Science, 2017, 26, 1692-1697.	3.1	7
123	Unanticipated Stickiness of α-Pinene. Journal of Physical Chemistry A, 2017, 121, 3239-3246.	1.1	14
124	Ultrathin dendrimer–graphene oxide composite film for stable cycling lithium–sulfur batteries. Proceedings of the National Academy of Sciences of the United States of America, 2017, 114, 3578-3583.	3.3	90
125	Characterization of Protein Tyrosine Phosphatase 1B Inhibition by Chlorogenic Acid and Cichoric Acid. Biochemistry, 2017, 56, 96-106.	1.2	18
126	The O <sub>2</sub> -Evolving Complex of Photosystem II: Recent Insights from Quantum Mechanics/Molecular Mechanics (QM/MM), Extended X-ray Absorption Fine Structure (EXAFS), and Femtosecond X-ray Crystallography Data. Accounts of Chemical Research, 2017, 50, 41-48.	7.6	168

#	Article	IF	CITATIONS
127	Thousandfold Enhancement of Photoreduction Lifetime in Re(bpy)(CO) <sub>3</sub> via Spin-Dependent Electron Transfer from a Perylenediimide Radical Anion Donor. Journal of the American Chemical Society, 2017, 139, 16466-16469.	6.6	20
128	On the relationship between cumulative correlation coefficients and the quality of crystallographic data sets. Protein Science, 2017, 26, 2410-2416.	3.1	7
129	Robust resistive memory devices using solution-processable metal-coordinated azoÂaromatics. Nature Materials, 2017, 16, 1216-1224.	13.3	244
130	Electronic π-Delocalization Boosts Catalytic Water Oxidation by Cu(II) Molecular Catalysts Heterogenized on Graphene Sheets. Journal of the American Chemical Society, 2017, 139, 12907-12910.	6.6	108
131	X-ray Free Electron Laser Radiation Damage through the S-State Cycle of the Oxygen-Evolving Complex of Photosystem II. Journal of Physical Chemistry B, 2017, 121, 9382-9388.	1.2	14
132	Crystallographic Data Support the Carousel Mechanism of Water Supply to the Oxygen-Evolving Complex of Photosystem II. ACS Energy Letters, 2017, 2, 2299-2306.	8.8	58
133	Linker Length-Dependent Electron-Injection Dynamics of Trimesitylporphyrins on SnO <sub>2</sub> Films. Journal of Physical Chemistry C, 2017, 121, 22690-22699.	1.5	13
134	Protospacer Adjacent Motif-Induced Allostery Activates CRISPR-Cas9. Journal of the American Chemical Society, 2017, 139, 16028-16031.	6.6	104
135	Antimony Complexes for Electrocatalysis: Activity of a Mainâ€Group Element in Proton Reduction. Angewandte Chemie, 2017, 129, 9239-9243.	1.6	12
136	Charge Transport and Rectification in Donor–Acceptor Dyads. Journal of Physical Chemistry C, 2017, 121, 19053-19062.	1.5	20
137	Tensor-Train Split-Operator Fourier Transform (TT-SOFT) Method: Multidimensional Nonadiabatic Quantum Dynamics. Journal of Chemical Theory and Computation, 2017, 13, 4034-4042.	2.3	84
138	Hard templating ultrathin polycrystalline hematite nanosheets: effect of nano-dimension on CO <sub>2</sub> to CO conversion via the reverse water-gas shift reaction. Nanoscale, 2017, 9, 12984-12995.	2.8	36
139	Interfacial Structure and Electric Field Probed by <i>in Situ</i> Electrochemical Vibrational Stark Effect Spectroscopy and Computational Modeling. Journal of Physical Chemistry C, 2017, 121, 18674-18682.	1.5	77
140	Characterization of ammonia binding to the second coordination shell of the oxygen-evolving complex of photosystem II. Dalton Transactions, 2017, 46, 16089-16095.	1.6	12
141	Electron Transfer Assisted by Vibronic Coupling from Multiple Modes. Journal of Chemical Theory and Computation, 2017, 13, 6000-6009.	2.3	41
142	Triplet–triplet energy transfer in artificial and natural photosynthetic antennas. Proceedings of the National Academy of Sciences of the United States of America, 2017, 114, E5513-E5521.	3.3	24
143	Thermodynamic and Structural Factors That Influence the Redox Potentials of Tungsten–Alkylidyne Complexes. ACS Catalysis, 2017, 7, 6134-6143.	5.5	7
144	Electrode-Ligand Interactions Dramatically Enhance CO <sub>2</sub> Conversion to CO by the [Ni(cyclam)](PF <sub>6</sub> ) <sub>2</sub> Catalyst. ACS Catalysis, 2017, 7, 5282-5288.	5.5	43

#	Article	IF	CITATIONS
145	A full set of iridium( <scp>iv</scp> ) pyridine-alkoxide stereoisomers: highly geometry-dependent redox properties. Chemical Science, 2017, 8, 1642-1652.	3.7	32
146	Is the Supporting Information the Venue for Reproducibility and Transparency?. Journal of Physical Chemistry A, 2017, 121, 9680-9681.	1,1	1
147	Is the Supporting Information the Venue for Reproducibility and Transparency?. Journal of Physical Chemistry C, 2017, 121, 28212-28213.	1.5	1
148	Is the Supporting Information the Venue for Reproducibility and Transparency?. Journal of Physical Chemistry B, 2017, 121, 11425-11426.	1.2	2
149	New Insights from Sum Frequency Generation Vibrational Spectroscopy into the Interactions of Islet Amyloid Polypeptides with Lipid Membranes. Journal of Diabetes Research, 2016, 2016, 1-17.	1.0	17
150	Heterogenized Iridium Water-Oxidation Catalyst from a Silatrane Precursor. ACS Catalysis, 2016, 6, 5371-5377.	5.5	79
151	Allosteric Pathways in the PPARÎ <sup>3</sup> -RXRα nuclear receptor complex. Scientific Reports, 2016, 6, 19940.	1.6	39
152	High-Potential Porphyrins Supported on SnO <sub>2</sub> and TiO <sub>2</sub> Surfaces for Photoelectrochemical Applications. Journal of Physical Chemistry C, 2016, 120, 28971-28982.	1.5	28
153	Ultraviolet vision: photophysical properties of the unprotonated retinyl Schiff base in the Siberian hamster cone pigment. Theoretical Chemistry Accounts, 2016, 135, 1.	0.5	5
154	Time-Sliced Thawed Gaussian Propagation Method for Simulations of Quantum Dynamics. Journal of Physical Chemistry A, 2016, 120, 3260-3269.	1.1	20
155	Solution Structures of Highly Active Molecular Ir Water-Oxidation Catalysts from Density Functional Theory Combined with High-Energy X-ray Scattering and EXAFS Spectroscopy. Journal of the American Chemical Society, 2016, 138, 5511-5514.	6.6	63
156	Fabrication of Modularly Functionalizable Microcapsules Using Protein-Based Technologies. ACS Biomaterials Science and Engineering, 2016, 2, 1856-1861.	2.6	23
157	Smelling Sulfur: Copper and Silver Regulate the Response of Human Odorant Receptor OR2T11 to Low-Molecular-Weight Thiols. Journal of the American Chemical Society, 2016, 138, 13281-13288.	6.6	60
158	Hot Hole Hopping in a Polyoxotitanate Cluster Terminated with Catechol Electron Donors. Journal of Physical Chemistry C, 2016, 120, 20006-20015.	1.5	14
159	Controlling the rectification properties of molecular junctions through molecule–electrode coupling. Nanoscale, 2016, 8, 16357-16362.	2.8	33
160	Formate to Oxalate: A Crucial Step for the Conversion of Carbon Dioxide into Multi arbon Compounds. ChemCatChem, 2016, 8, 3453-3457.	1.8	24
161	Organometallic Iridium Complex Containing a Dianionic, Tridentate, Mixed Organic–Inorganic Ligand. Inorganic Chemistry, 2016, 55, 8121-8129.	1.9	4
162	Fundamental Role of Oxygen Stoichiometry in Controlling the Band Gap and Reactivity of Cupric Oxide Nanosheets. Journal of the American Chemical Society, 2016, 138, 10978-10985.	6.6	39

#	Article	IF	CITATIONS
163	Ammonia Binding in the Second Coordination Sphere of the Oxygen-Evolving Complex of Photosystem II. Biochemistry, 2016, 55, 4432-4436.	1.2	14
164	Role of Tensorial Electronic Friction in Energy Transfer at Metal Surfaces. Physical Review Letters, 2016, 116, 217601.	2.9	85
165	Ferroceneâ€Promoted Longâ€Cycle Lithium–Sulfur Batteries. Angewandte Chemie, 2016, 128, 15038-15042.	1.6	11
166	Ferroceneâ€Promoted Longâ€Cycle Lithium–Sulfur Batteries. Angewandte Chemie - International Edition, 2016, 55, 14818-14822.	7.2	46
167	Allosteric Communication Disrupted by a Small Molecule Binding to the Imidazole Glycerol Phosphate Synthase Protein–Protein Interface. Biochemistry, 2016, 55, 6484-6494.	1.2	33
168	<i>Ab initio</i> tensorial electronic friction for molecules on metal surfaces: Nonadiabatic vibrational relaxation. Physical Review B, 2016, 94, .	1.1	74
169	Dissecting Dynamic Allosteric Pathways Using Chemically Related Small-Molecule Activators. Structure, 2016, 24, 1155-1166.	1.6	38
170	Electrochemical CO <sub>2</sub> Reduction to Hydrocarbons on a Heterogeneous Molecular Cu Catalyst in Aqueous Solution. Journal of the American Chemical Society, 2016, 138, 8076-8079.	6.6	450
171	Quantitative structure-property relationship model leading to virtual screening of fullerene derivatives: Exploring structural attributes critical for photoconversion efficiency of polymer solar cell acceptors. Nano Energy, 2016, 26, 677-691.	8.2	25
172	Sum Frequency Generation Spectroscopy and Molecular Dynamics Simulations Reveal a Rotationally Fluid Adsorption State of α-Pinene on Silica. Journal of Physical Chemistry C, 2016, 120, 12578-12589.	1.5	29
173	Surface-Induced Anisotropic Binding of a Rhenium CO <sub>2</sub> -Reduction Catalyst on Rutile TiO <sub>2</sub> (110) Surfaces. Journal of Physical Chemistry C, 2016, 120, 20970-20977.	1.5	44
174	Molecular design of light-harvesting photosensitizers: effect of varied linker conjugation on interfacial electron transfer. Physical Chemistry Chemical Physics, 2016, 18, 18678-18682.	1.3	21
175	Structure–function relationships in single molecule rectification by N-phenylbenzamide derivatives. New Journal of Chemistry, 2016, 40, 7373-7378.	1.4	7
176	Assessment of DFT for Computing Sum Frequency Generation Spectra of an Epoxydiol and a Deuterated Isotopologue at Fused Silica/Vapor Interfaces. Journal of Physical Chemistry B, 2016, 120, 1919-1927.	1.2	17
177	S <sub>3</sub> State of the O <sub>2</sub> -Evolving Complex of Photosystem II: Insights from QM/MM, EXAFS, and Femtosecond X-ray Diffraction. Biochemistry, 2016, 55, 981-984.	1.2	62
178	Experimental and Theoretical Study of CO <sub>2</sub> Insertion into Ruthenium Hydride Complexes. Inorganic Chemistry, 2016, 55, 1623-1632.	1.9	42
179	Ultrafast Photoinduced Interfacial Proton Coupled Electron Transfer from CdSe Quantum Dots to 4,4′-Bipyridine. Journal of the American Chemical Society, 2016, 138, 884-892.	6.6	52
180	Molecular titanium–hydroxamate complexes as models for TiO <sub>2</sub> surface binding. Chemical Communications, 2016, 52, 2972-2975.	2.2	30

#	Article	IF	CITATIONS
181	Facile solvolysis of a surprisingly twisted tertiary amide. New Journal of Chemistry, 2016, 40, 1974-1981.	1.4	3
182	Orientation of Cyano-Substituted Bipyridine Re(I) <i>fac</i> -Tricarbonyl Electrocatalysts Bound to Conducting Au Surfaces. Journal of Physical Chemistry C, 2016, 120, 1657-1665.	1.5	46
183	Analysis of the Radiation-Damage-Free X-ray Structure of Photosystem II in Light of EXAFS and QM/MM Data. Biochemistry, 2015, 54, 1713-1716.	1.2	73
184	Crucial Role of Nuclear Dynamics for Electron Injection in a Dye–Semiconductor Complex. Journal of Physical Chemistry Letters, 2015, 6, 2393-2398.	2.1	49
185	Implausibility of the vibrational theory of olfaction. Proceedings of the National Academy of Sciences of the United States of America, 2015, 112, E2766-74.	3.3	76
186	Facet-Dependent Photoelectrochemical Performance of TiO <sub>2</sub> Nanostructures: An Experimental and Computational Study. Journal of the American Chemical Society, 2015, 137, 1520-1529.	6.6	242
187	Steered Quantum Dynamics for Energy Minimization. Journal of Physical Chemistry B, 2015, 119, 715-727.	1.2	3
188	Accurate Line Shapes from Sub-1 cm <sup>–1</sup> Resolution Sum Frequency Generation Vibrational Spectroscopy of α-Pinene at Room Temperature. Journal of Physical Chemistry A, 2015, 119, 1292-1302.	1.1	49
189	Computational Insights on Crystal Structures of the Oxygen-Evolving Complex of Photosystem II with Either Ca <sup>2+</sup> or Ca <sup>2+</sup> Substituted by Sr <sup>2+</sup> . Biochemistry, 2015, 54, 820-825.	1.2	31
190	Electrochemical Reduction of Aqueous Imidazolium on Pt(111) by Proton Coupled Electron Transfer. Topics in Catalysis, 2015, 58, 23-29.	1.3	14
191	Intramolecular Proton Transfer Boosts Water Oxidation Catalyzed by a Ru Complex. Journal of the American Chemical Society, 2015, 137, 10786-10795.	6.6	246
192	Reply to Turin et al.: Vibrational theory of olfaction is implausible. Proceedings of the National Academy of Sciences of the United States of America, 2015, 112, E3155.	3.3	19
193	Correlating Photoacidity to Hydrogen-Bond Structure by Using the Local O–H Stretching Probe in Hydrogen-Bonded Complexes of Aromatic Alcohols. Journal of Physical Chemistry A, 2015, 119, 4800-4812.	1.1	26
194	Behavior of the Ru-bda Water Oxidation Catalyst Covalently Anchored on Glassy Carbon Electrodes. ACS Catalysis, 2015, 5, 3422-3429.	5.5	78
195	Stable Iridium(IV) Complexes of an Oxidation-Resistant Pyridine-Alkoxide Ligand: Highly Divergent Redox Properties Depending on the Isomeric Form Adopted. Journal of the American Chemical Society, 2015, 137, 7243-7250.	6.6	51
196	Interfacial electron transfer in photoanodes based on phosphorus(v) porphyrin sensitizers co-deposited on SnO2 with the Ir(III)Cp* water oxidation precatalyst. Journal of Materials Chemistry A, 2015, 3, 3868-3879.	5.2	47
197	Characterization of Parallel β-Sheets at Interfaces by Chiral Sum Frequency Generation Spectroscopy. Journal of Physical Chemistry Letters, 2015, 6, 1310-1315.	2.1	30
198	Triplet Oxygen Evolution Catalyzed by a Biomimetic Oxomanganese Complex: Functional Role of the Carboxylate Buffer. ACS Catalysis, 2015, 5, 2384-2390.	5.5	15

#	Article	IF	CITATIONS
199	Beyond Local Group Modes in Vibrational Sum Frequency Generation. Journal of Physical Chemistry A, 2015, 119, 3407-3414.	1.1	18
200	Activation of OR1A1 suppresses PPAR-Î <sup>3</sup> expression by inducing HES-1 in cultured hepatocytes. International Journal of Biochemistry and Cell Biology, 2015, 64, 75-80.	1.2	54
201	NH <sub>3</sub> Binding to the S <sub>2</sub> State of the O <sub>2</sub> -Evolving Complex of Photosystem II: Analogue to H <sub>2</sub> O Binding during the S <sub>2</sub> → S <sub>3</sub> Transition. Biochemistry, 2015, 54, 5783-5786.	1.2	68
202	Preparation of Halogenated Fluorescent Diaminophenazine Building Blocks. Journal of Organic Chemistry, 2015, 80, 9881-9888.	1.7	14
203	Computational Design of Intrinsic Molecular Rectifiers Based on Asymmetric Functionalization of <i>N</i> -Phenylbenzamide. Journal of Chemical Theory and Computation, 2015, 11, 5888-5896.	2.3	34
204	Mechanism of Manganese-Catalyzed Oxygen Evolution from Experimental and Theoretical Analyses of <sup>18</sup> 0 Kinetic Isotope Effects. ACS Catalysis, 2015, 5, 7104-7113.	5.5	41
205	Unusual kinetics of thermal decay of dim-light photoreceptors in vertebrate vision. Proceedings of the National Academy of Sciences of the United States of America, 2014, 111, 10438-10443.	3.3	27
206	A Selfâ€Improved Waterâ€Oxidation Catalyst: Is One Site Really Enough?. Angewandte Chemie - International Edition, 2014, 53, 205-209.	7.2	82
207	Linker Rectifiers for Covalent Attachment of Transitionâ€Metal Catalysts to Metalâ€Oxide Surfaces. ChemPhysChem, 2014, 15, 1138-1147.	1.0	20
208	MoD-QM/MM Structural Refinement Method: Characterization of Hydrogen Bonding in the <i>Oxytricha nova</i> G-Quadruplex. Journal of Chemical Theory and Computation, 2014, 10, 5125-5135.	2.3	16
209	Structural Changes in the Oxygen-Evolving Complex of PhotosystemÂll Induced by the S <sub>1</sub> to S <sub>2</sub> Transition: A Combined XRD and QM/MM Study. Biochemistry, 2014, 53, 6860-6862.	1.2	46
210	QM/MM Model of the Mouse Olfactory Receptor MOR244-3 Validated by Site-Directed Mutagenesis Experiments. Biophysical Journal, 2014, 107, L5-L8.	0.2	32
211	Single Molecule Rectification Induced by the Asymmetry of a Single Frontier Orbital. Journal of Chemical Theory and Computation, 2014, 10, 3393-3400.	2.3	36
212	High-Conductance Conformers in Histograms of Single-Molecule Current–Voltage Characteristics. Journal of Physical Chemistry C, 2014, 118, 8316-8321.	1.5	12
213	Theoretical EXAFS studies of a model of the oxygenâ€evolving complex of photosystem II obtained with the quantum cluster approach. International Journal of Quantum Chemistry, 2013, 113, 474-478.	1.0	26
214	S <sub>0</sub> -State Model of the Oxygen-Evolving Complex of Photosystem II. Biochemistry, 2013, 52, 7703-7706.	1.2	97
215	Efficiency of Interfacial Electron Transfer from Zn-Porphyrin Dyes into TiO <sub>2</sub> Correlated to the Linker Single Molecule Conductance. Journal of Physical Chemistry C, 2013, 117, 24462-24470.	1.5	55
216	Ultrafast Solventâ€Assisted Electronic Level Crossing in 1â€Naphthol. Angewandte Chemie - International Edition, 2013, 52, 6871-6875.	7.2	24

#	Article	IF	CITATIONS
217	Functional Role of Pyridinium during Aqueous Electrochemical Reduction of CO <sub>2</sub> on Pt(111). Journal of Physical Chemistry Letters, 2013, 4, 745-748.	2.1	146
218	Hydroxamate Anchors for Improved Photoconversion in Dye-Sensitized Solar Cells. Inorganic Chemistry, 2013, 52, 6752-6764.	1.9	102
219	Electrostatic Effects on Proton Coupled Electron Transfer in Oxomanganese Complexes Inspired by the Oxygen-Evolving Complex of Photosystem II. Journal of Physical Chemistry B, 2013, 117, 6217-6226.	1.2	36
220	Computational Studies of the Oxygen-Evolving Complex of Photosystem II and Biomimetic Oxomanganese Complexes for Renewable Energy Applications. ACS Symposium Series, 2013, , 203-215.	0.5	1
221	Chiral Sum Frequency Generation for In Situ Probing Proton Exchange in Antiparallel β-Sheets at Interfaces. Journal of the American Chemical Society, 2013, 135, 3592-3598.	6.6	74
222	Innenrücktitelbild: Ultrafast Solvent-Assisted Electronic Level Crossing in 1-Naphthol (Angew. Chem.) Tj ETQqC	0 0 rgBT 1.6	Oyerlock 10
223	Chapter 1. Inverse molecular design for materials discovery. Chemical Modelling, 2013, , 1-31.	0.2	4
224	Tunneling through Coulombic barriers: quantum control of nuclear fusion. Molecular Physics, 2012, 110, 995-999.	0.8	3
225	Orientation of a Series of CO2 Reduction Catalysts on Single Crystal TiO2 Probed by Phase-Sensitive Vibrational Sum Frequency Generation Spectroscopy (PS-VSFG). Journal of Physical Chemistry C, 2012, 116, 24107-24114.	1.5	48
226	Light-driven water oxidation for solar fuels. Coordination Chemistry Reviews, 2012, 256, 2503-2520.	9.5	337
227	A tridentate Ni pincer for aqueous electrocatalytic hydrogen production. New Journal of Chemistry, 2012, 36, 1149.	1.4	88
228	Fuel selection for a regenerative organic fuel cell/flow battery: thermodynamic considerations. Energy and Environmental Science, 2012, 5, 9534.	15.6	35
229	Ultrafast Vibrational Frequency Shifts Induced by Electronic Excitations: Naphthols in Low Dielectric Media. Journal of Physical Chemistry A, 2012, 116, 2775-2790.	1.1	29
230	Kepler Predictor–Corrector Algorithm: Scattering Dynamics with One-Over-R Singular Potentials. Journal of Chemical Theory and Computation, 2012, 8, 24-35.	2.3	3
231	Amphiphilic Adsorption of Human Islet Amyloid Polypeptide Aggregates to Lipid/Aqueous Interfaces. Journal of Molecular Biology, 2012, 421, 537-547.	2.0	71
232	Bioinspired High-Potential Porphyrin Photoanodes. Journal of Physical Chemistry C, 2012, 116, 4892-4902.	1.5	69
233	Reduction of Systematic Uncertainty in DFT Redox Potentials of Transition-Metal Complexes. Journal of Physical Chemistry C, 2012, 116, 6349-6356.	1.5	145
234	Allosteric pathways in imidazole glycerol phosphate synthase. Proceedings of the National Academy of Sciences of the United States of America, 2012, 109, E1428-36.	3.3	192

#	Article	IF	CITATIONS
235	The O–H Stretching Mode of a Prototypical Photoacid as a Local Dielectric Probe. Journal of Physical Chemistry A, 2011, 115, 10511-10516.	1.1	15
236	Inverse Design and Synthesis of acac-Coumarin Anchors for Robust TiO <sub>2</sub> Sensitization. Journal of the American Chemical Society, 2011, 133, 9014-9022.	6.6	79
237	S <sub>1</sub> -State Model of the O <sub>2</sub> -Evolving Complex of Photosystem II. Biochemistry, 2011, 50, 6308-6311.	1.2	210
238	Structural–Functional Role of Chloride in Photosystem II. Biochemistry, 2011, 50, 6312-6315.	1.2	132
239	Covalent Attachment of a Rhenium Bipyridyl CO <sub>2</sub> Reduction Catalyst to Rutile TiO <sub>2</sub> . Journal of the American Chemical Society, 2011, 133, 6922-6925.	6.6	106
240	Water-stable, hydroxamate anchors for functionalization of TiO2 surfaces with ultrafast interfacial electron transfer. Energy and Environmental Science, 2010, 3, 917.	15.6	99
241	Characterization of Proton Coupled Electron Transfer in a Biomimetic Oxomanganese Complex: Evaluation of the DFT B3LYP Level of Theory. Journal of Chemical Theory and Computation, 2010, 6, 755-760.	2.3	61
242	Visible Light Sensitization of TiO <sub>2</sub> Surfaces with Alq3 Complexes. Journal of Physical Chemistry C, 2010, 114, 1317-1325.	1.5	37
243	Deposition of an oxomanganese water oxidation catalyst on TiO2 nanoparticles: computational modeling, assembly and characterization. Energy and Environmental Science, 2009, 2, 230.	15.6	80
244	Quantum Dynamics of the Excitedâ€State Intramolecular Proton Transfer in 2â€{2‪â€Hydroxyphenyl)benzothiazole. Israel Journal of Chemistry, 2009, 49, 187-197.	1.0	10
245	Coherent Control of Quantum Dynamics with Sequences of Unitary Phase-Kick Pulses. Annual Review of Physical Chemistry, 2009, 60, 293-320.	4.8	35
246	Hydroxamate anchors for water-stable attachment to TiO2 nanoparticles. Energy and Environmental Science, 2009, 2, 1173.	15.6	91
247	Energy Flow Under Control. Science, 2009, 326, 245-246.	6.0	5
248	Computational insights into the O2-evolving complex of photosystem II. Photosynthesis Research, 2008, 97, 91-114.	1.6	62
249	A Model of the Oxygen-Evolving Center of Photosystem II Predicted by Structural Refinement Based on EXAFS Simulations. Journal of the American Chemical Society, 2008, 130, 6728-6730.	6.6	110
250	Acetylacetonate Anchors for Robust Functionalization of TiO <sub>2</sub> Nanoparticles with Mn(II)â^'Terpyridine Complexes. Journal of the American Chemical Society, 2008, 130, 14329-14338.	6.6	151
251	Quantum Mechanics/Molecular Mechanics Study of the Catalytic Cycle of Water Splitting in Photosystem II. Journal of the American Chemical Society, 2008, 130, 3428-3442.	6.6	345
252	QM/MM computational studies of substrate water binding to the oxygen-evolving centre of photosystem II. Philosophical Transactions of the Royal Society B: Biological Sciences, 2008, 363, 1149-1156.	1.8	70

#	Article	IF	CITATIONS
253	Multiple unitary-pulses for coherent-control of tunnelling and decoherence. Journal of Modern Optics, 2007, 54, 2617-2627.	0.6	3
254	Ultrafast Photooxidation of Mn(II)â^'Terpyridine Complexes Covalently Attached to TiO <sub>2</sub> Nanoparticles. Journal of Physical Chemistry C, 2007, 111, 11982-11990.	1.5	82
255	The MP/SOFT methodology for simulations of quantum dynamics: Model study of the photoisomerization of the retinyl chromophore in visual rhodopsin. Journal of Photochemistry and Photobiology A: Chemistry, 2007, 190, 274-282.	2.0	16
256	A Self-Consistent Space-Domain Decomposition Method for QM/MM Computations of Protein Electrostatic Potentials. Journal of Chemical Theory and Computation, 2006, 2, 175-186.	2.3	47
257	Computational Studies of the Primary Phototransduction Event in Visual Rhodopsin. Accounts of Chemical Research, 2006, 39, 184-193.	7.6	75
258	QM/MM Models of the O2-Evolving Complex of Photosystem II. Journal of Chemical Theory and Computation, 2006, 2, 1119-1134.	2.3	136
259	Characterization of synthetic oxomanganese complexes and the inorganic core of the O2-evolving complex in photosystem II: Evaluation of the DFT/B3LYP level of theory. Journal of Inorganic Biochemistry, 2006, 100, 786-800.	1.5	99
260	Matching-pursuit/split-operator-Fourier-transform simulations of excited-state nonadiabatic quantum dynamics in pyrazine. Journal of Chemical Physics, 2006, 125, 124313.	1.2	61
261	Model study of coherent quantum dynamics of hole states in functionalized semiconductor nanostructures. Journal of Chemical Physics, 2005, 122, 154709.	1.2	43
262	QM/MM Study of the NMR Spectroscopy of the Retinyl Chromophore in Visual Rhodopsin. Journal of Chemical Theory and Computation, 2005, 1, 674-685.	2.3	45
263	Influence of Thermal Fluctuations on Interfacial Electron Transfer in Functionalized TiO2 Semiconductors. Journal of the American Chemical Society, 2005, 127, 18234-18242.	6.6	196
264	Model Study of Coherent-Control of the Femtosecond Primary Event of Vision. Journal of Physical Chemistry B, 2004, 108, 6745-6749.	1.2	32
265	Quantum tunneling dynamics in multidimensional systems: A matching-pursuit description. Journal of Chemical Physics, 2004, 121, 1676-1680.	1.2	50
266	QM/MM Study of Energy Storage and Molecular Rearrangements Due to the Primary Event in Vision. Biophysical Journal, 2004, 87, 2931-2941.	0.2	98
267	Matching-pursuit for simulations of quantum processes. Journal of Chemical Physics, 2003, 118, 6720-6724.	1.2	77
268	Quantum Dynamics Simulations of Interfacial Electron Transfer in Sensitized TiO2Semiconductors. Journal of the American Chemical Society, 2003, 125, 7989-7997.	6.6	368
269	Coherent Control in the Presence of Intrinsic Decoherence: Proton Transfer in Large Molecular Systems. Physical Review Letters, 2002, 89, 143201.	2.9	51
270	Real time path integrals using the Herman–Kluk propagator. Journal of Chemical Physics, 2002, 116, 2748-2756.	1.2	53

#	Article	IF	CITATIONS
271	Semiclassical Molecular Dynamics Simulations of the Excited State Photodissociation Dynamics of H2O in the A1B1Bandâ€. Journal of Physical Chemistry B, 2002, 106, 8271-8277.	1.2	7
272	Nonadiabatic photodissociation dynamics of ICN in the $\tilde{A}f$ continuum: A semiclassical initial value representation study. Journal of Chemical Physics, 2000, 112, 5566-5575.	1.2	65
273	Semiclassical molecular dynamics simulations of intramolecular proton transfer in photoexcited 2-(2′-hydroxyphenyl)–oxazole. Journal of Chemical Physics, 2000, 113, 9510-9522.	1.2	59
274	Semiclassical molecular dynamics simulations of excited state double-proton transfer in 7-azaindole dimers. Journal of Chemical Physics, 1999, 110, 9922-9936.	1.2	138
275	Femtosecond photoelectron spectroscopy of the I2â^ anion: A semiclassical molecular dynamics simulation method. Journal of Chemical Physics, 1999, 110, 3736-3747.	1.2	84
276	Semiclassical molecular dynamics simulations of ultrafast photodissociation dynamics associated with the Chappuis band of ozone. Journal of Chemical Physics, 1998, 108, 498-510.	1.2	65